Available online at www.sciencedirect.com
ScienceDirect
Antiviral Research 76 (2007) 48–58
Antiviral Research
www.elsevier.com/locate/antiviral

Inhibition of hepatitis C virus p7 membrane channels in a liposome-based assay system

Corine StGelais, Tobias J. Tuthill, Dean S. Clarke, David J. Rowlands, Mark Harris, Stephen Griffin *

Institute of Molecular and Cellular Biology, Faculty of Biological Sciences and Astbury Centre for Structural Molecular Biology, University of Leeds, Leeds LS2 9JT, United Kingdom

Received 29 January 2007; accepted 9 May 2007

Abstract

Chemotherapy for patients chronically infected with hepatitis C virus (HCV) is ineffective in over 50% of cases, generating a high demand for new drug targets. The p7 protein of HCV displays membrane channel activity *in vitro* and is essential for replication *in vivo* though its precise role in the virus life cycle is unknown. p7 channel activity can be specifically inhibited by several classes of compounds, making this protein an attractive candidate for drug development, though techniques used to date in characterising this protein are unsuited to compound library screening. Here we describe an assay for the channel forming ability of p7 based on the release of a fluorescent indicator from liposomes. We show that recombinant p7 from genotype 1b HCV causes a dose-dependent release of dye when mixed with liposomes and that this property is enhanced at acidic pH. We demonstrate that this activity is due to the formation of a size-selective pore rather than non-specific disruption of liposomes and that activity can be blocked by amantadine and several other compounds, validating it as a measure of p7 channel function. This system provides the first convenient *in vitro* assay for exploiting p7 as a therapeutic target.

Keywords: Hepatitis C virus; p7; Amantadine; Ion channel; Viroporin; Liposome permeability

1. Introduction

Hepatitis C virus (HCV) currently infects ∼170 million people world-wide, causing widespread morbidity and mortality. It has replaced alcohol abuse as the leading indicator for liver transplantation and causes 10,000 deaths per year in the USA alone. The majority of carriers are unaware of their positive status due to mainly asymptomatic acute disease followed by persistence in over 80% of infections, resulting in severe disease manifestations such as cirrhosis or hepatocellular carcinoma decades after exposure. No vaccine exists and intervention is limited to the use of antivirals in the form of interferon α combined with ribavirin. Despite improvements such as the use of pegylated interferon for sustained dosing, this therapy is effective in only ∼50% of cases, making the development of new anti-HCV therapies paramount. In particular, infections with HCV genotype 1 are associated with a high level of resistance to therapy and more aggressive forms of disease (Pawlotsky, 2000; Simmonds, 2004). Interestingly, recent clinical trials where amantadine has been included alongside current protocols have given encouraging, though controversial, results in the re-treatment of patients failing conventional therapy: most often those infected with genotype 1 HCV (Deltenre et al., 2004; Mangia et al., 2004).

HCV is the prototype member of the *Hepacivirus* genus of the Flaviviridae (Choo et al., 1992; Simmonds et al., 2005). It is an enveloped virus with a positive sense RNA genome of ∼9.6 kb that encodes a single polyprotein of ∼3000 amino acids that is translated from an internal ribosome entry site (IRES) at the 5′ end of the genome. The polyprotein is subsequently cleaved by host signalases and viral proteases to yield 10 mature virus gene products (Lohmann et al., 1996), comprising the virus structural proteins involved in particle formation and non-structural proteins which are concerned with replication of the viral genome (Egger et al., 2002; Moradpour et al., 2003).

It is unknown whether or not HCV p7 is a virion component. It is a small hydrophobic protein of 63 amino acids and contains two trans-membrane alpha helices separated by a conserved basic loop (Lin et al., 1994; Mizushima et al., 1994;

* Corresponding author. Tel.: +44 113 343 8217; fax: +44 113 343 5638.
E-mail address: bmbsdcg@bmb.leeds.ac.uk (S. Griffin).

0166-3542/$ – see front matter © 2007 Elsevier B.V. All rights reserved.
doi:10.1016/j.antiviral.2007.05.001

Carrere-Kremer et al., 2002). We previously showed that purified recombinant p7 displayed amantadine-sensitive membrane channel activity in artificial bilayers (Griffin et al., 2003). Other investigators have since confirmed these findings using synthetic p7 peptides and identified alternative inhibitors, namely long alkyl chain imino-sugar derivatives (Pavlovic et al., 2003) and hexamethylene amiloride (HMA) (Premkumar et al., 2004). It is not known where in the HCV life cycle p7 functions, though importantly it is necessary for HCV replication in chimpanzees (Sakai et al., 2003) and the homologous protein of the related bovine viral diarrhoea virus (BVDV) is required for the production of infectious virus in cell culture (Harada et al., 2000).

p7 belongs to a group of viral proteins known as viroporins which includes the M2 ion channel of influenza A virus (IAV) (Gonzalez and Carrasco, 2003). M2 is also amantadine sensitive and the drug and its derivatives are used clinically (Hay et al., 1985; Ciampor et al., 1992; Duff and Ashley, 1992; Wang et al., 1993). We demonstrated that p7 from genotype 1 HCV could function in a cellular assay measuring M2-dependent transport of the IAV haemagglutinin (Sakaguchi et al., 1996) to the cell surface and that amantadine also inhibited p7 in this context (Griffin et al., 2004). Amantadine also blocks the p7 protein (Ghibaudo et al., 2004; Takikawa et al., 2006) of HCV's closest relative, GB virus B (GBV-B) *in vitro*, though it has little effect on virus secretion or infectivity in culture (Premkumar et al., 2006). The ambiguity surrounding p7 inhibitors combined with controversial clinical trial data on inclusion of amantadine alongside interferon α and ribavirin highlights the need for a robust *in vitro* assay for the identification of candidate inhibitors of p7 from different virus genotypes. Here, we describe an assay for p7 function based on its ability to effect release of the fluorophore carboxyfluorescein (CF) from liposomes. The system provides a convenient initial screen for identifying candidate p7 inhibitors for subsequent testing in cell culture assays that is readily adaptable to higher throughput formats in the future.

2. Materials and methods

2.1. GST-FLAG-p7 protein expression and purification

Plasmid pGEX6FLAGp7 encoding a glutathione-*S*-transferase (GST)-FLAG-p7 fusion protein was expressed in *E. coli* BL21 (DE3), cleaved using recombinant rhinovirus 14 3C protein and FLAG-p7 then purified by HPLC as described previously (Clarke et al., 2006). Protein concentration was determined by absorbance at 280 nm and lyophilised protein stored at −80 °C prior to being dissolved in methanol or in SDS-PAGE sample buffer for liposome assays or gel analysis, respectively.

2.2. Preparation of unilamellar lipid vesicles

Lipids were purchased in chloroform from Avanti Polar Lipids Inc. (Birmingham, AL). One milligram per milliliter of L-α-phosphatidic acid (egg monosodium salt) (PA) and L-α-phosphatidylcholine acid (egg) (PC) with a final concentration of 0.5% (w/w) L-α-phosphatidylethanolamine with lissamine rhodamine B labelled head groups, was dried under a stream of argon to form a film on the bottom of a glass tube, then placed under vacuum for 2 h. An appropriate volume of buffer to give a liposome concentration of 1 mg/ml containing carboxyfluorescein (CF) (Sigma-Aldrich) at a self-quenching concentration (50 mM CF in HEPES buffered saline (HBS): 10 mM HEPES-NaOH pH 7.4, 107 mM NaCl) was used to re-hydrate the lipids with vigorous shaking at room temperature (RT) overnight. Alternatively, buffer containing 0.5 mM FITC-conjugated dextrans (FD) of molecular weights of 4 kDa (FD-4), 10 kDa (FD-10), and 70 kDa (FD-70) (Sigma) was used for experiments estimating p7 pore size. Unilamellar liposomes were produced by extrusion through a 0.4 μm Nucleopore Track-Etch membrane filter (Whatman), using an Avanti mini-extruder with Hamilton glass syringes. Liposomes were purified by centrifugation at 100,000 × *g* for 20 min in a Sorvall S55S ultra centrifuge rotor incorporating three wash steps and finally resuspended in HBS. Liposomes were freshly prepared for each experiment.

2.3. Liposome permeability assays

Release of vesicular contents into the medium was assessed using the quenching properties of CF. Permeability induced by FLAG-p7 was assessed by incubating protein (typically 5 μg determined by $A_{280\,nm}$, dissolved in methanol) with 50 μM concentration of liposomes (determined by rhodamine absorbance at 570 nm). The total reaction volume was made up to 100 μl with HBS, giving a p7 concentration of ∼50 nM. Fluorescence measurements were performed in a FLUOstar OPTIMA microplate reader (BMG technologies) with excitation and emission set at 485 and 520 nm, respectively. As expected due to the large separation of absorption/emission spectra, no bleed-through of rhodamine fluorescence from the liposomes was detectable using these parameters (data not shown). Real-time measurement of CF release was performed using 10 nM of the bee venom peptide, mellitin (Sigma) as a positive control. Fluorescence values were read every 30 s for 1 h at 37 °C, except in HMA inhibition assays where data was collected for 30 min (see below). All samples were repeated in triplicate and averaged. Initial rates were calculated from the slope of the linear part of the curve for the first 6 min of each experiment and expressed as change in arbitrary fluorescence units per second ($\Delta FU\ s^{-1}$).

Assays for the effect of pH on CF release or experiments with FD could not be performed in real time due to the quenching effect of pH on CF fluorescence and the lower concentration of fluorophores used respectively. Instead, samples were incubated at 37 °C for 1 h, then centrifuged at 160,000 × *g* for 20 min in an S100-AT3 rotor (Sorvall) to pellet the liposomes and the resulting supernatant transferred to a 96-well micro titre plate and normalised to 0.5% (w/v) Triton X-100 prior to fluorimetry. For FD experiments, background fluorescence (0%) corresponded to spontaneous leakage from vesicle only controls and 100% leakage was taken as the fluorescence value obtained after addition of 0.5% (v/v) Triton X-100 to liposomes prior to centrifugation. The degree of permeabilisation was calculated from the equation: $\%\text{leakage} = ((F_f - F_0)/(F_{100} - F_0)) \times 100$ where F_f is the

fluorescence determined after the addition of protein, F_0 is the initial fluorescence of liposomes alone and F_{100} is the fluorescence value after the addition of Triton X-100. All samples were repeated in triplicate and averaged.

For experiments assessing the effect of pH on CF release, liposomes containing CF were resuspended in citrate/phosphate buffers (citric acid and sodium phosphate dibasic ($12H_2O$) mixed appropriately to give pH 6.8, 6.2, 5.4 and 4.8). Following separation of liposomes and supernatant by centrifugation, pH was re-adjusted to 7.4 by the addition of buffering amounts of 1 M Tris–HCl pH 8.0 as judged by the restoration of 100% fluorescence in Triton X-100 lysed controls of the same volume (Fig. 4A).

2.4. Ficoll density separation of liposome-incorporated FLAG-p7

FLAG-p7 (5 μg) was mixed with liposomes as described above and incubated for 1 h at 37 °C. The reaction was then mixed with an equal volume of 40% (w/v) Ficoll (Sigma) in HBS, giving a final concentration of 20% (w/v) Ficoll. This was placed in the bottom of a 2.2 ml ultra centrifuge tube and 1.7 ml of a 10% (w/v) Ficoll solution was layered over the top followed by 0.3 ml of HBS. The gradient was then centrifuged at 100,000 × *g* for 30 min in a S55S rotor (Sorvall). Eight × 275 μl fractions were collected and 20 μl analysed by SDS-PAGE followed by immunoblot. A 50 μl sample was also tested for rhodamine fluorescence, measured at λ_{ex} 520 nm and λ_{em} 570 nm, to detect liposomes.

2.5. Inhibition of FLAG-p7 induced membrane permeability

Inhibition assays were carried out as described above except for the addition of each antiviral compound to 1 μM as indicated prior to incubation at 37 °C. Compounds used were amantadine hydrochloride (Sigma), rimantadine (kindly provided by Helen Bright, GSK), hexamethylene amiloride (HMA, Sigma) and three compounds provided by GSK, termed: GSK-1, GSK-2 and GSK-3. The structures of these compounds are protected by GSK patent and cannot be disclosed due to conflicting commercial interest. Amantadine-HCl was stored at 4 °C as a 10 mM stock solution in water. Other compounds were stored as 40 mM stock solutions in DMSO at −20 °C. Assays performed using HMA were performed using revised standard conditions involving a 30 min time course, and were detected using an updated FLUOStar Optima machine thus yielding slightly different arbitrary fluorescence values. Initial rates were, however, directly comparable with previous assays.

2.6. Antibodies and immunoblot analysis

Antibody 1055 is an affinity-purified rabbit polyclonal antibody raised against the C-terminus of p7 and has been described previously (Griffin et al., 2005). 1055 was used at 1/1000 dilution in immunoblot analysis. FLAG-tagged protein was detected using a mouse monoclonal antibody, M2 (Sigma-Aldrich) at a 1/20,000 dilution. Immunoblot analysis was carried out as described previously (Clarke et al., 2006).

3. Results

3.1. Purified FLAG-p7 protein associates with liposomes

Before testing the effects of FLAG-p7 on liposome permeability, it was necessary to demonstrate specific association of purified FLAG-p7 with liposomes. FLAG-p7 was purified by HPLC following cleavage of GST-FLAG-p7 using recombinant rhinovirus (type 14) 3C protease as previously described (Clarke et al., 2006). Fig. 1A shows 10 μg purified protein stained with Coomassie Brilliant Blue (Fig. 1A, left panel) and immunoblotted using the p7-specific antibody 1055, which reveals the presence of higher molecular weight oligomeric forms of the protein (Fig. 1A, right panel), as a result of the anionic SDS present within sample buffer. These are not present in solution, with their formation being detergent/lipid dependent and mediated by the p7 moiety (Clarke et al., 2006). Our previous investigations have also ruled out the formation of micellar aggregates by both FLAG-p7 and GST-fusion protein precursors in aqueous solution: oligomeric forms of these proteins were detectable only when chemically cross-linked in the presence of SDS or lipids (Griffin et al., 2003; Clarke et al., 2006).

Purified FLAG-p7 protein was incubated with 50 μM liposomes at 37 °C for 1 h prior to flotation on a discontinuous Ficoll density gradient to separate liposomes from aqueous reaction mixtures. Gradient fractions were analysed by immunoblotting to detect FLAG-p7 and the distribution of liposomes followed by rhodamine fluorescence (Fig. 1B). Estimates from immunoblots indicated that approximately 25% of the FLAG-p7 added to the reaction had associated with the liposome fraction, as judged by co-migration with the peak of rhodamine fluorescence (Fig. 1B, estimated by comparing protein in fraction 7 with that in fractions 1 and 2). Control flotations containing no liposomes indicated that FLAG-p7 did not migrate non-specifically to the 10% Ficoll/aqueous interface (Fig. 1B, middle panel).

3.2. FLAG-p7 causes a dose-dependent release of CF from liposomes

Increasing concentrations of purified FLAG-p7 were incubated with 50 μM liposomes containing 50 mM CF and release was monitored over a period of 60 min by fluorimetry. The bee venom peptide mellitin was included as a positive control for CF release as it has been well characterised in such assays. In the absence of FLAG-p7 or in solvent controls, baseline levels of CF fluorescence were observed due to the quenching properties of CF at the concentrations present within the liposomes (Fig. 2A, blue and black traces), although a small increase in fluorescence occurred gradually over time; most likely a result of liposome fusion events. Addition of increasing concentrations of FLAG-p7 promoted a rapid, dose-dependent release of CF into the aqueous milieu leading to a loss of self-quenching and resultant fluorescent signal (Fig. 2A). The larger increase in both the initial rate (Fig. 2A, right hand panel) and the overall levels

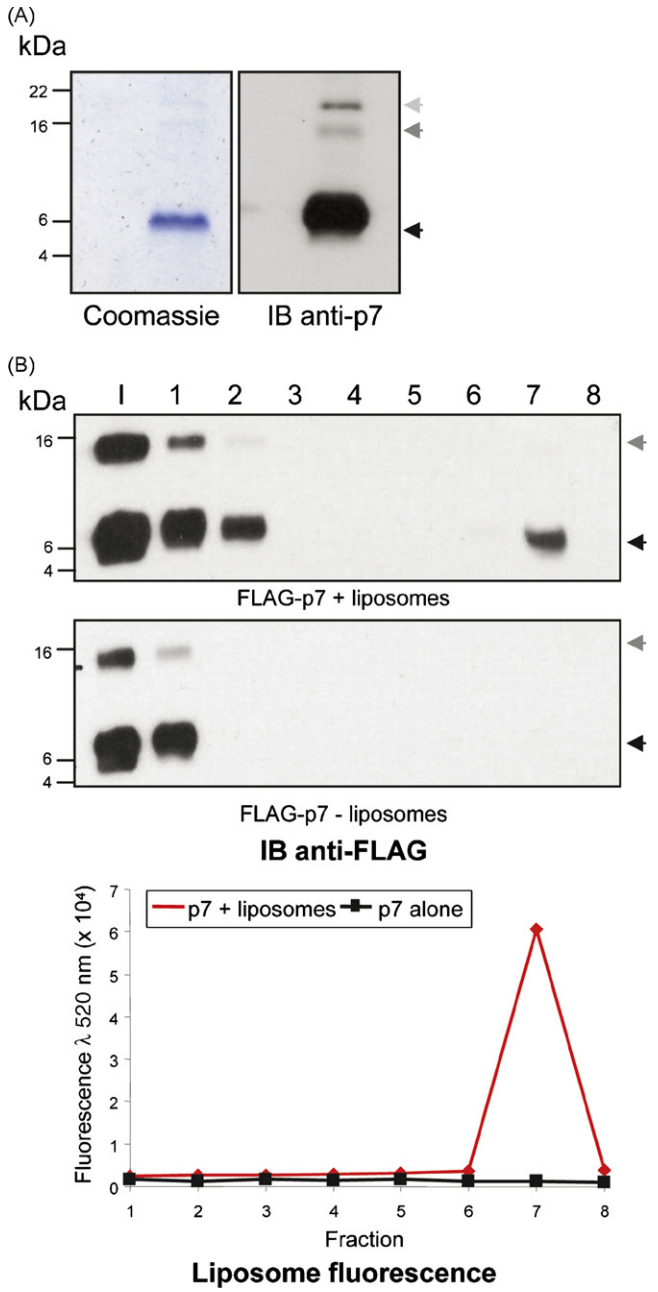

Fig. 1. Association of purified FLAG-p7 with liposomes. Ficoll density gradient separation was used to demonstrate association of purified FLAG-p7 with liposomes. (A) Ten microgram of purified FLAG-p7 was analysed by SDS-PAGE and Coomassie staining (left panel) or immunoblot with p7-specific antibody, 1055 (right panel). In addition to monomeric FLAG-p7 (black arrow), higher molecular weight forms were evident (lighter arrows) representing oligomers of p7 formed in the presence of SDS micelles. (B) Five microgram of purified FLAG-p7 was mixed with PA:PC liposomes, adjusted to 20% Ficoll and layered at the bottom of a discontinuous density gradient then subjected to ultracentrifugation. Eight equal fractions (lanes 1, bottom-8, top) were taken from the gradient and 20 μl aliquots analysed by immunoblot (top panel) using an anti-FLAG monoclonal antibody alongside 10% of the input (I). Again, as well as monomeric FLAG-p7 (black arrow) higher molecular weight forms were detected with increased protein concentration (lighter arrow). In addition, a sample was removed from fractions for fluorimetric detection of rhodamine-labelled liposomes to confirm migration to the 10% Ficoll/aqueous interface (bottom panel, red trace). Control reactions where no liposomes were added resulted in FLAG-p7 remaining at the bottom of the gradient (middle panel and bottom panel, black trace). (For interpretation of the references to colour in this figure legend, the reader is referred to the web version of the article.)

of CF release from the addition of 25 and 10 nM protein compared with the difference between 50 and 25 nM suggests that FLAG-p7 was required above a certain threshold concentration for efficient dye release to occur (Fig. 2A).

To ensure that dye release was being mediated by FLAG-p7 and not trace contaminants remaining following HPLC or a non-specific effect of adding protein to the liposomes, the un-cleaved parental GST-FLAG-p7 fusion protein purified by the same process was added to liposomes at the same concentration (Fig. 2B). This caused no specific CF release compared to solvent or liposome controls (Fig. 2B, purple trace) and this is consistent with our previous observation that this GST-fusion protein forms channels very inefficiently in black lipid membrane (BLM) systems (Griffin et al., 2003). This important control further demonstrates the absence of soluble micellar aggregates, which are a concern when amphipathic protein sequences are added to liposome suspensions and could potentially disrupt membranes resulting in dye release in a non-specific fashion.

The reproducibility of CF release for multiple batches of purified FLAG-p7 mixed with fresh liposome preparations was then assessed to ensure the suitability of the assay for potential high-throughput formats. Fig. 2C shows initial rates from six representative experiments, each displaying similar kinetics for FLAG-p7-mediated release of CF in the range of 29–37 RFU/s with no statistically significant differences.

3.3. *Purified FLAG-p7 forms channels with defined radius when inserted into liposomes*

To ensure that release of CF was due to the formation of a discrete channel structure rather than a potential non-specific disruption of membranes by the amphipathic *trans*-membrane alpha helices of p7, liposomes containing fluorescently labelled dextrans (FD) of increasing molecular weight were incubated with protein and liposome-depleted supernatants assessed by fluorimetry (Fig. 3). Mellitin was also included as this has previously been shown to form channels with defined size constraints (Ladokhin et al., 1997; Park et al., 2006). FD with molecular weight of 4 kDa (FD-4) (Stokes' radius of ∼14 Å) was released efficiently from liposomes upon addition of mellitin or FLAG-p7 (Fig. 3). Release of FD-10 (Stokes' radius of ∼23 Å), however, was significantly reduced for both proteins (Fig. 3), indicating inefficient transport of molecules of this size, and was further reduced for FD-70 (Stokes' radius of ∼60 Å) (Fig. 3). The release of FD-70 by both mellitin and FLAG-p7 in these assays likely reflects either non-specific escape of FD or release via liposome fusion events over the 60 min incubation period. This assumption is supported by the fact that there is no statistically significant difference in release of FD-70 (Fig. 3) or indeed a larger dextran FD-250 (data not shown) by the two proteins (mellitin and FLAG-p7). These data are consistent with the notion that FLAG-p7, like mellitin, forms channels in the membrane of defined size and stoichiometry as we have observed previously (Griffin et al., 2003; Clarke et al., 2006). Furthermore, these data are consistent with our estimates of p7 channel size being up to 5 nm diameter, with a lumen of 2 nm diameter or less (Griffin et al., 2003).

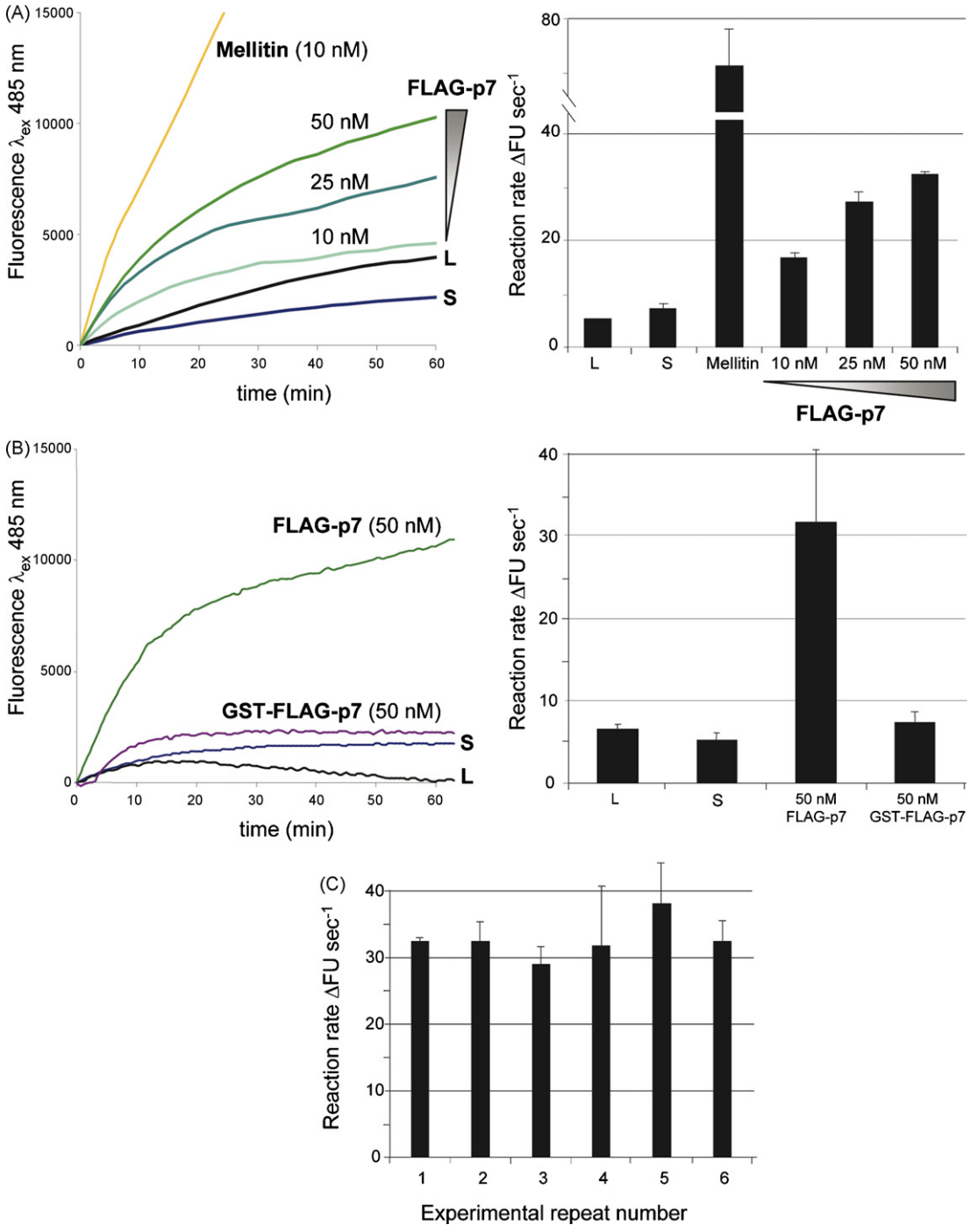

Fig. 2. Dose-dependent release of CF from liposomes by addition of FLAG-p7. FLAG-p7/liposome mixes were monitored in real time for CF release by fluorimetry at λ_{ex} 485 nm/λ_{em} 520 nm. (A) Dose-dependent release of CF caused by increasing amounts of FLAG-p7 shown in real time (left hand panel) and by initial rate calculated from the linear part of the curve (right hand panel). (B) Comparison of FLAG-p7-mediated CF release with that caused by addition of parental GST-FLAG-p7 fusion protein to the same concentration. (C) Assessment of reproducibility for FLAG-p7-mediated CF release. Initial rates for CF release were calculated for six batches of purified FLAG-p7 protein, each mixed with freshly prepared liposomes in triplicate. L: CF release from liposomes alone; S: CF release from liposomes where same volume of methanol was added as a solvent control; ΔFU s^{-1}: change in arbitrary fluorescence units/second. Error bars represent standard deviation of the mean.

3.4. FLAG-p7 has an increased effect on liposome permeability at acidic pH

Given that p7 can substitute for M2 in a cell-based assay in an amantadine-sensitive fashion (Griffin et al., 2004), the effect of pH on the ability of FLAG-p7 to permeabilise liposomes was investigated. Lowered pH, however, reduces CF fluorescence (Fig. 4A) preventing real-time assessment of FLAG-p7 activity, therefore liposomes were pelleted and experiments normalised to the value obtained by Triton X-100 lysis following restoration of neutral pH. The effect of pH on CF fluorescence and its recovery by the addition of quenching amounts of neutral buffer

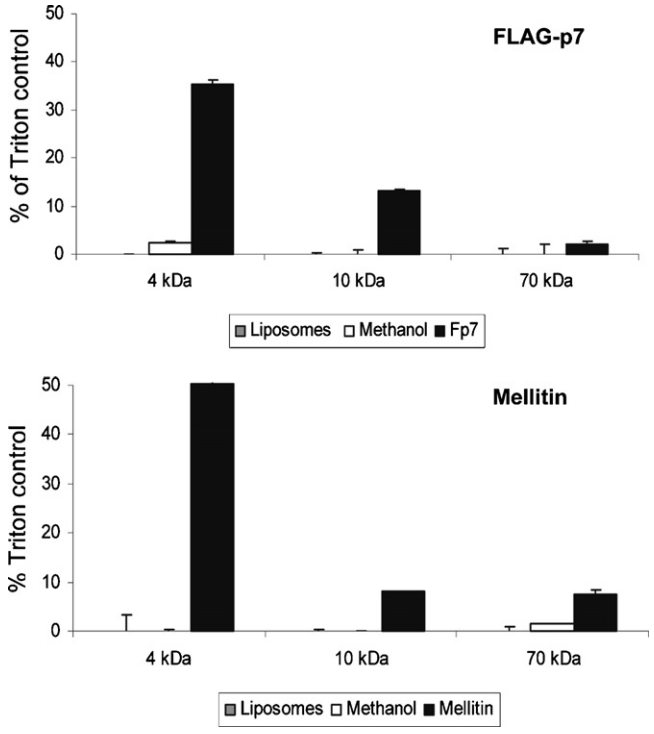

Fig. 3. FLAG-p7 displays size constraints for transport of fluorescent dextrans (FD). The ability of FLAG-p7 and mellitin to effect release of increasing molecular weight fluorescent dextrans from liposomes was assessed using fluorimetry at λ_{ex} 485 nm/λ_{em} 520 nm on liposome-free supernatants (normalised for each dextran to Triton X-100 lysed liposomes as 100% reading) after incubation at 37 °C for 1 h. Top panel: 50 nM FLAG-p7 with 4 kDa dextran (FD-4), 10 kDa dextran (FD-10), 70 kDa dextran (FD-70); bottom panel shows results for 10 nM mellitin. Negative controls for liposomes alone (taken as 0%) and where methanol was added as a solvent control are also shown for each FD. Error bars represent standard deviation of the mean.

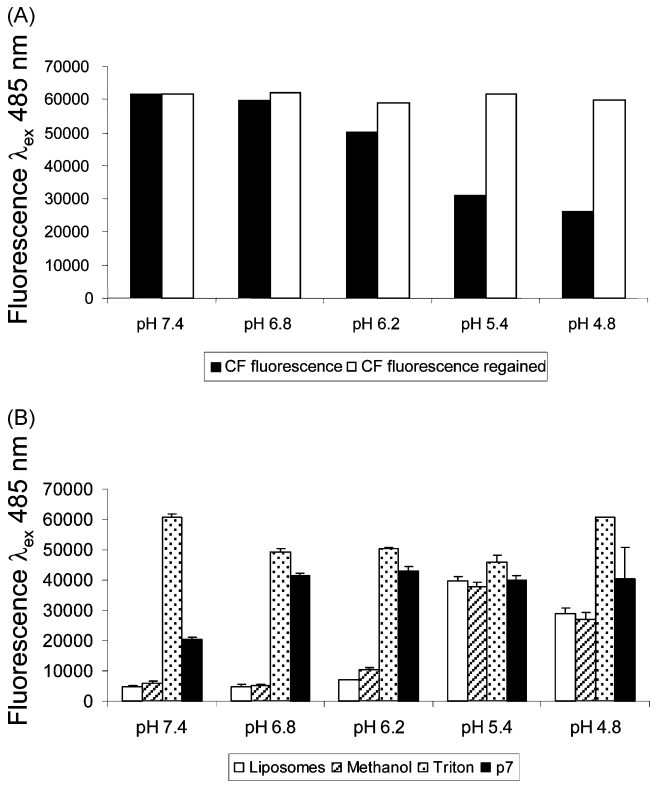

Fig. 4. Enhanced FLAG-p7-mediated membrane permeability at reduced pH. To assess the effect of pH on FLAG-p7-induced CF release, protein and liposomes were incubated in buffers of reduced pH at 37 °C for 1 h. Liposome-free supernatants were then re-adjusted to pH 7.4 by the addition of quenching amounts of 1 M Tris–HCl pH 8.0 to restore CF fluorescence. (A) Restoration of CF fluorescence in solution following treatment at acidic pH as indicated by addition of neutral buffer. (B) FLAG-p7 (50 nM) mediated CF release from liposomes at acidic pH following restoration of CF fluorescence with Triton X-100 lysed liposomes as positive and methanol solvent plus liposome only negative controls. Error bars represent standard deviation of the mean.

was first determined (Fig. 4A). Satisfied that CF fluorescence could be successfully restored, permeability assays using 50 nM FLAG-p7 were performed in buffers of increasingly acidic pH (Fig. 4B). Normalisation of pH revealed a specific increase in permeability upon addition of FLAG-p7 at pH 6.8 and 6.2 relative to the standard assay conditions (Fig. 4B). Unfortunately, pH < 6.0 appeared to disrupt liposome integrity causing a non-specific release of CF into the supernatant making it impossible to assess FLAG-p7 permeability under these conditions. Due to the inability to follow the reaction in real time at acidic pH, however, it was decided to continue to use the assay under standard conditions at pH 7.4. In addition, although dilute CF solutions obtained following release from liposomes into supernatants remain soluble despite fluorescence quenching at lowered pH, 50 mM CF used in generating liposome stocks cannot be prepared at pH < 7.4, thus making lower pH buffers unsuitable for the standard assay conditions.

3.5. Screening of p7 inhibitors in liposome permeability assays

Since we first demonstrated the inhibitory action of amantadine, other classes of inhibitors have been shown to abrogate p7 ion channel activity in BLM systems (Griffin et al., 2003; Pavlovic et al., 2003; Premkumar et al., 2004). To assess whether p7 was similarly inhibited in the liposome system and validate it as a rapid screening system for p7 inhibitors, we first assessed the ability of amantadine (Fig. 5), and other candidate compounds (Fig. 6) to block FLAG-p7-mediated release of CF from liposomes at a concentration of 1 μM, as this concentration is known to effectively block single channels in BLM systems (Griffin et al., 2003). Controls in which inhibitors were incubated with liposomes in the absence of FLAG-p7 showed no adverse effects on liposome stability and their addition to the mellitin-positive control had no effect on CF release, indicating that the compounds did not prevent permeability by non-specifically coating liposomes (data not shown). Surprisingly, amantadine at 1 μM did not completely block CF release, yet titrating increasing amounts reduced both the initial rates and overall quantity of CF released over the assay period. From these titration experiments, we determined that, for a FLAG-p7 concentration of 50 nM, the IC_{50} for amantadine was ~2 μM.

Next, we compared the effects of amantadine with its methylated derivative, rimantadine, HMA and also three experimental compounds: GSK-1, GSK-2 and GSK-3 (Fig. 6). Both the real-time traces and graphs of initial rates showed that at a

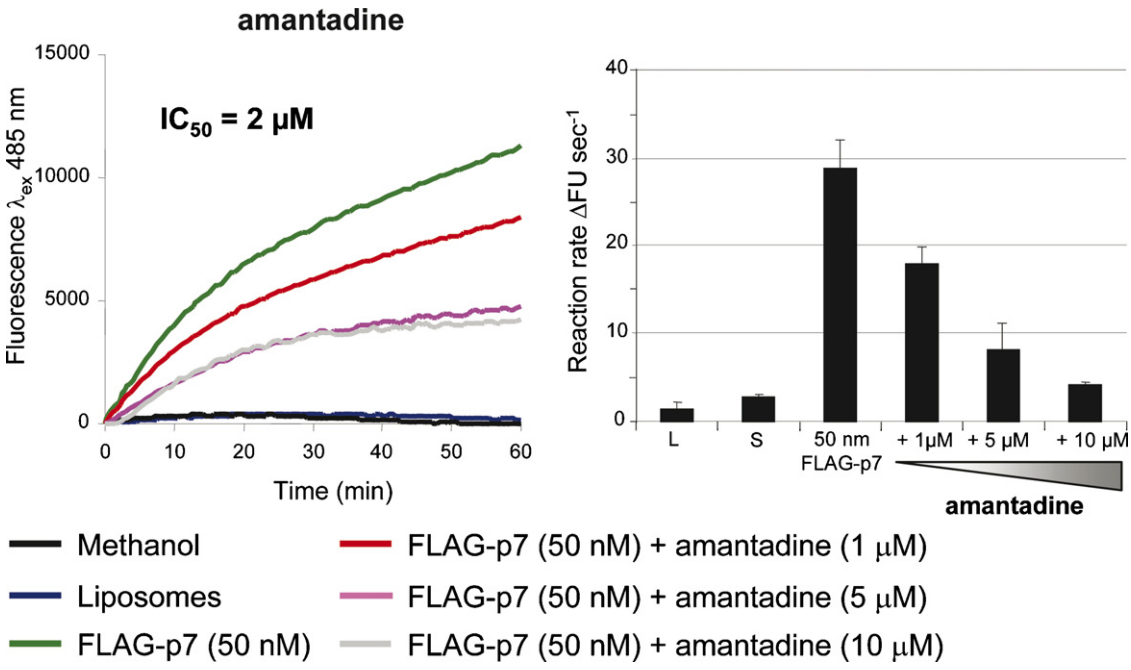

Fig. 5. Inhibition of FLAG-p7-mediated CF release by amantadine. To validate the liposome assay as a means of screening p7 inhibitors, amantadine was titrated into reactions containing 50 nM FLAG and CF release monitored in real time by fluorimetry at λ_{ex} 485 nm/λ_{em} 520 nm. Initial rates of CF release were calculated from the linear portions of resultant curves (right panel) and used to calculate an IC_{50} for amantadine for this concentration of FLAG-p7 as ~2 μM. Traces summarised in key at bottom. $\Delta FU\ s^{-1}$: change in arbitrary fluorescence units/second. Error bars represent standard deviation of the mean.

concentration of 1 μM, rimantadine, HMA, GSK-1 and GSK-2 specifically inhibited FLAG-p7-mediated CF release from liposomes (Fig. 6A–D, red trace), whereas GSK-3 had no effect (Fig. 6E, red trace). Differences in efficacy were most evident by comparison of initial rates for each compound (Fig. 6F), which confirm amantadine as being less effective at this concentration than the other active compounds; rimantadine, HMA and GSK-2 being most effective. This assay was therefore capable of discerning the relative efficacies of specific inhibitors from non-functional compounds in a system that allows assessment of multiple candidates in parallel.

4. Discussion

We describe here the first assay for screening inhibitors of p7 ion channel function which bypasses the need for slow and labour-intensive BLM systems which are limited in both reproducibility and the number of compounds that can be tested in parallel. Key to the success of the system is the ability to express and purify p7 from bacteria using a GST-fusion methodology, which can be readily scaled up to produce large quantities of authentic p7 protein and avoids the problems associated with synthesis of this highly hydrophobic peptide sequence (Griffin et al., 2003; Clarke et al., 2006). Furthermore, the simplicity of the assay renders it amenable to medium/high-throughput screening systems.

The liposome assay would appear upon first inspection to have limited relevance to the physiological function of p7. Our previous studies and the data presented here, however, suggest that p7 forms channel structures in liposomes equivalent to those seen in cells. We have previously demonstrated that both GST-FLAG-p7 fusion protein and cleaved FLAG-p7 are capable of oligomerising in liposomes to produce structures with a heptameric stoichiometry and that the channels formed are cation selective in BLM (Clarke et al., 2006). In this study, we again demonstrated specific association of FLAG-p7 with liposomes and showed that the resultant channel structures were limited for the Stokes' radius of fluorescent substrate to which they were permeable. Not all of the FLAG-p7 was able to insert itself into the membrane, which is unsurprising in the absence of the cellular machinery usually required for this process to occur. Interestingly, we have shown that p7 is still membrane-associated in cells when expressed without its upstream signal peptide (Griffin et al., 2005) and related proteins have also been shown to insert into membranes spontaneously (Agirre et al., 2002). It is unlikely that the liposome concentration is limiting for protein insertion in these experiments as both the mellitin and Triton X-100 positive controls released far more CF into the supernatant than FLAG-p7. Furthermore, the relationship between FLAG-p7 concentration and release of CF implied a threshold below which channel structures might not efficiently form, consistent with a two-step kinetic involving first membrane insertion and subsequent assembly of channel structures for efficient CF release. The size limit of FD able to be efficiently released by FLAG-p7 (between 14 and 23 Å) indicates the formation of defined channel structures and is comparable to estimates of the sizes of lumen in heptameric structures formed by both GST-FLAG-p7 and FLAG-p7 we have observed in TEM and biochemical studies (Griffin et al., 2003; Clarke et al., 2006). It is, therefore, unlikely that CF release is merely a

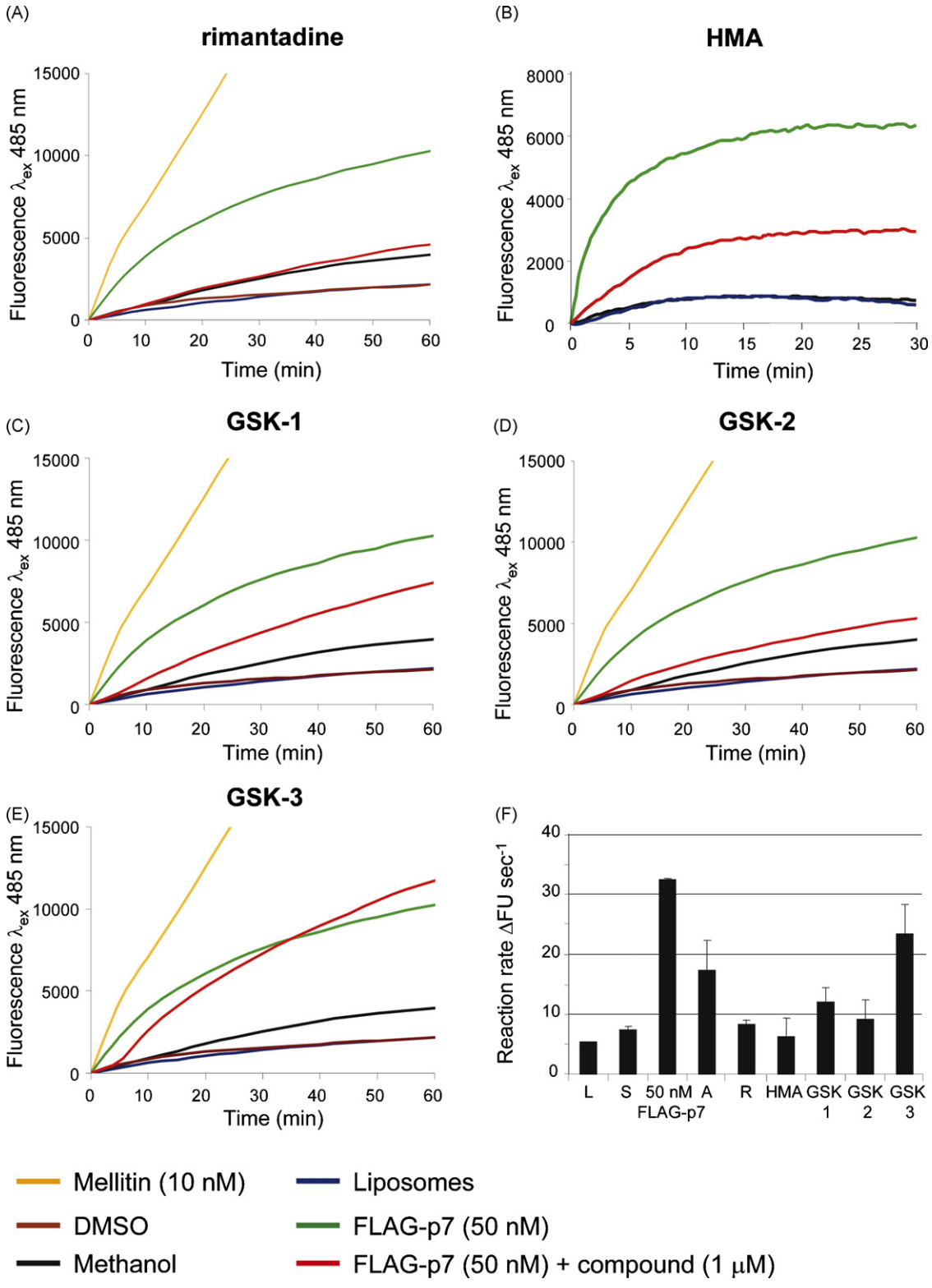

Fig. 6. Effects of candidate p7 inhibitors on FLAG-p7-mediated CF release. The ability of 50 nM FLAG-p7 to cause release of CF in the presence of 1 μM candidate inhibitory compounds (red trace) was assessed in real time by fluorimetry at λ_{ex} 485 nm/λ_{em} 520 nm. Traces summarised in key at bottom left. (A) Rimantadine. (B) HMA (NB: see Section 2). (C) GSK-1. (D) GSK-2. (E) GSK-3. (F) Plot of initial rates for FLAG-p7-mediated CF release in presence/absence of potential inhibitory compounds. ΔFU s^{-1}: change in arbitrary fluorescence units/second. Error bars represent standard deviation of the mean.

function of non-specific disruption of membranes by the amphipathic alpha helices present within p7 and in fact reflects a true channel-forming activity.

A concern when adding amphipathic proteins to aqueous liposome suspensions is the potential for them to form micellar aggregates that could non-specifically disrupt membranes. Unincorporated FLAG-p7, therefore, has the potential to act in this fashion, yet evidence from this, and previous studies, indicates that this is not the case. Micellar aggregates are, by definition, oligomeric, yet the detection of oligomeric forms of p7 in solution required the presence of either lipid or anionic detergents (Griffin et al., 2003; Clarke et al., 2006). Furthermore, mellitin is also highly amphipathic and is added to such systems in excess, yet is well documented to effect specific dye release and the GST-FLAG-p7 precursor protein caused no detectable release of CF above background. Lastly, CF release mediated by such structures acting in a detergent-like fashion would not be expected to show specific sensitivity to certain channel-blocking compounds. The unincorporated protein present within these assays, therefore, is inconsequential and does not require removal; indeed, such a step would greatly reduce the suitability of the system for potential high-throughput screening.

The increase in FLAG-p7-mediated release of CF at a lower pH suggests that p7 channels may be gated by acidic pH and facilitate the transport of protons in a similar fashion to M2 (Wang et al., 1995; Chizhmakov et al., 1996; Pinto et al., 1997; Okada et al., 2001). Although no measurement of proton transport was undertaken in these studies, the increased amount of CF liberated is suggestive of increased opening of p7 channel structures. Given that p7 exhibits an eight-fold preference for cations over anions in bilayer systems (Pavlovic et al., 2003; Premkumar et al., 2004; Clarke et al., 2006), the increase in anionic CF release could actually represent a far greater degree of channel opening in response to relatively minor changes in pH. Transport of protons by p7 would be consistent with our observation that the protein could substitute for M2 in a cellular assay measuring the transport of pH-sensitive haemagglutinin to the cell surface (Griffin et al., 2004) and could have implications for the role of p7 in the HCV life cycle. It is widely accepted that p7 is most likely involved in HCV assembly, and given the sensitivity of both JFH-1 (Lindenbach et al., 2005; Wakita et al., 2005; Zhong et al., 2005) derived cell culture virus and retrovirus particles pseudotyped with HCV glycoproteins to low pH (Bartosch et al., 2003; Hsu et al., 2003; Tscherne et al., 2006), equalisation of pH gradients during virus assembly by p7 would be a conceivable role for this protein in replication.

The liposome permeability assay is the third experimental system we have used to demonstrate the ability of amantadine to inhibit the function of p7 from genotype 1b HCV (Griffin et al., 2003, 2004; Clarke et al., 2006), yet the efficacy of this drug in clinical trials is a subject of much controversy. Studies comparing the results of multiple trials have suggested that any possible effect amantadine may have is confined to the treatment of genotype 1 infected individuals that have previously failed dual therapy (Deltenre et al., 2004; Mangia et al., 2004). Certainly, amantadine alone or in dual combination with interferon α has no effect on clinical outcome (Gaeta et al., 2001; Muzi et al., 2005). Although nothing is known about the ability of amantadine to reach the liver or enter hepatocytes at the doses used in these trials, it seems that its efficacy is confined to a small number of cases and may indeed be limited genetically to 1b subtype viruses (Mihm et al., 2006). Evidence from a recent study implies that amantadine resistance arises rapidly during the course of therapy, as is the case for IAV (Maynard et al., 2006) and this may mask antiviral activity early in treatment. Amantadine also inhibits the p7 protein of GBV-B, HCV's closest relative, *in vitro*, yet appears to have little effect on virus spread in culture (Premkumar et al., 2006). During the preparation of this manuscript, however, a report detailing apparent amantadine sensitivity in culture of both genotype 2a JFH-1 and an infectious chimera containing the p7 protein from the genotype 1b Australia isolate was published (Haqshenas et al., 2006). Conversely, however, the authors also demonstrated that the Australia p7 protein itself was insensitive to amantadine in BLM experiments. These data do not tally with our own observations for JFH-1 infectivity, and we have also observed that JFH-1 p7 is insensitive to amantadine *in vitro* though it remains sensitive to related compounds. The sensitivity of p7 from multiple HCV genotypes, both in our liposome system and in culture, will be reported elsewhere (Griffin et al., manuscript in preparation).

Interestingly, in the liposome system, the effects of amantadine on CF release were modest compared with, for example, rimantadine which reduced dye release to that of solvent controls at 1 μM. This shows an advantage of the system over BLM where this concentration of amantadine completely blocks the activity of single p7 channels (Griffin et al., 2003; Clarke et al., 2006). By assessing the effects of compounds on populations of p7 channels, the liposome assay appears to allow more broad-ranging comparisons of relative efficacy. The demonstration that HMA also blocked FLAG-p7-mediated CF release in this system to a similar level as rimantadine validates this assay as a means to test the effects of compounds proposed to block p7. Relative estimates of the potency of a compound can be derived from this assay by comparing both the initial rates of CF release (Figs. 2, 5 and 6) and the overall level of CF release; estimates of compound IC_{50} can also be derived from titration experiments.

5. Conclusions

A limiting factor for many HCV drug development studies has been the inability to test against multiple viral genotypes. Variation in p7 sequence, in particular in those residues lining the hydrophilic face of the N terminal alpha helix which is thought to comprise the inner surface of the lumen (Carrere-Kremer et al., 2002; Patargias et al., 2006), could explain both the ineffectiveness of amantadine in clinical trials as well as the insensitivity of JFH-1 HCV to the drug in culture. We have begun to assess p7 proteins from other HCV genotypes in the liposome system and early results do indeed indicate genotype-specific differences in susceptibility of p7 to inhibitory compounds. The liposome permeability assay will permit the testing of novel p7 inhibitors against multiple HCV genotypes and provides the first potential means to develop p7 library screens on a medium/high-throughput scale.

Acknowledgements

We thank Helen Bright and Tony Carroll (Virology, GSK, Stevenage, UK) for experimental compounds GSK-1–3 and Arie Geerlof (University of Oxford, UK) for providing bacterial expression constructs for recombinant rhinovirus (type 14) 3C protein. SG was supported by the Wellcome Trust (Grant no. 074023) and TT by the Medical Research Council (Grant no. 63271). CStG was the recipient of a Cooperative Awards in Science and Engineering (CASE) PhD studentship from the Biotechnology and Biological Sciences Research Council and Pfizer, and DC a PhD studentship from the Medical Research Council.

References

Agirre, A., Barco, A., Carrasco, L., Nieva, J.L., 2002. Viroporin-mediated membrane permeabilization. Pore formation by nonstructural poliovirus 2B protein. J. Biol. Chem. 277, 40434–40441.

Bartosch, B., Vitelli, A., Granier, C., Goujon, C., Dubuisson, J., Pascale, S., Scarselli, E., Cortese, R., Nicosia, A., Cosset, F.L., 2003. Cell entry of hepatitis C virus requires a set of co-receptors that include the CD81 tetraspanin and the SR-B1 scavenger receptor. J. Biol. Chem. 278, 41624–41630.

Carrere-Kremer, S., Montpellier-Pala, C., Cocquerel, L., Wychowski, C., Penin, F., Dubuisson, J., 2002. Subcellular localization and topology of the p7 polypeptide of hepatitis C virus. J. Virol. 76, 3720–3730.

Chizhmakov, I.V., Geraghty, F.M., Ogden, D.C., Hayhurst, A., Antoniou, M., Hay, A.J., 1996. Selective proton permeability and pH regulation of the influenza virus M2 channel expressed in mouse erythroleukaemia cells. J. Physiol. 494, 329–336.

Choo, Q.L., Kuo, G., Weiner, A., Wang, K.S., Overby, L., Bradley, D., Houghton, M., 1992. Identification of the major, parenteral non-A, non-B hepatitis agent (hepatitis C virus) using a recombinant cDNA approach. Semin. Liver Dis. 12, 279–288.

Ciampor, F., Bayley, P.M., Nermut, M.V., Hirst, E.M., Sugrue, R.J., Hay, A.J., 1992. Evidence that the amantadine-induced, M2-mediated conversion of influenza A virus hemagglutinin to the low pH conformation occurs in an acidic trans Golgi compartment. Virology 188, 14–24.

Clarke, D., Griffin, S., Beales, L., Gelais, C.S., Burgess, S., Harris, M., Rowlands, D., 2006. Evidence for the formation of a heptameric ion channel complex by the hepatitis C virus p7 protein in vitro. J. Biol. Chem. 281, 37057–37068.

Deltenre, P., Henrion, J., Canva, V., Dharancy, S., Texier, F., Louvet, A., De Maeght, S., Paris, J.C., Mathurin, P., 2004. Evaluation of amantadine in chronic hepatitis C: a meta-analysis. J. Hepatol. 41, 462–473.

Duff, K.C., Ashley, R.H., 1992. The transmembrane domain of influenza A M2 protein forms amantadine-sensitive proton channels in planar lipid bilayers. Virology 190, 485–489.

Egger, D., Wolk, B., Gosert, R., Bianchi, L., Blum, H.E., Moradpour, D., Bienz, K., 2002. Expression of hepatitis C virus proteins induces distinct membrane alterations including a candidate viral replication complex. J. Virol. 76, 5974–5984.

Gaeta, G.B., Stornaiuolo, G., Stanzione, M., Ascione, T., Pasquazzi, C., Taliani, G., Cimino, L., Budillon, G., Piccinino, F., 2001. Interferon-alpha plus amantadine in chronic hepatitis C resistant to interferon alone: a pilot randomized study. J. Viral Hepat. 8, 284–286.

Ghibaudo, D., Cohen, L., Penin, F., Martin, A., 2004. Characterization of GB virus B polyprotein processing reveals the existence of a novel 13-kDa protein with partial homology to hepatitis C virus p7 protein. J. Biol. Chem. 279, 24965–24975.

Gonzalez, M.E., Carrasco, L., 2003. Viroporins. FEBS Lett. 552, 28–34.

Griffin, S.D., Beales, L.P., Clarke, D.S., Worsfold, O., Evans, S.D., Jaeger, J., Harris, M.P., Rowlands, D.J., 2003. The p7 protein of hepatitis C virus forms an ion channel that is blocked by the antiviral drug, amantadine. FEBS Lett. 535, 34–38.

Griffin, S.D., Harvey, R., Clarke, D.S., Barclay, W.S., Harris, M., Rowlands, D.J., 2004. A conserved basic loop in hepatitis C virus p7 protein is required for amantadine-sensitive ion channel activity in mammalian cells but is dispensable for localization to mitochondria. J. Gen. Virol. 85, 451–461.

Griffin, S., Clarke, D., McCormick, C., Rowlands, D., Harris, M., 2005. Signal peptide cleavage and internal targeting signals direct the hepatitis C virus p7 protein to distinct intracellular membranes. J. Virol. 79, 15525–15536.

Haqshenas, G., Dong, X., Ewart, G., Bowden, S., Gowans, E.J., 2006. A 2a/1b full-length p7 inter-genotypic chimeric genome of hepatitis C virus is infectious in vitro. Virology 360, 17–26.

Harada, T., Tautz, N., Thiel, H.J., 2000. E2-p7 region of the bovine viral diarrhea virus polyprotein: processing and functional studies. J. Virol. 74, 9498–9506.

Hay, A.J., Wolstenholme, A.J., Skehel, J.J., Smith, M.H., 1985. The molecular basis of the specific anti-influenza action of amantadine. EMBO J. 4, 3021–3024.

Hsu, M., Zhang, J., Flint, M., Logvinoff, C., Cheng-Mayer, C., Rice, C.M., McKeating, J.A., 2003. Hepatitis C virus glycoproteins mediate pH-dependent cell entry of pseudotyped retroviral particles. Proc. Natl. Acad. Sci. U. S. A. 100, 7271–7276.

Ladokhin, A.S., Selsted, M.E., White, S.H., 1997. Sizing membrane pores in lipid vesicles by leakage of co-encapsulated markers: pore formation by melittin. Biophys. J. 72, 1762–1766.

Lin, C., Lindenbach, B.D., Pragai, B.M., McCourt, D.W., Rice, C.M., 1994. Processing in the hepatitis C virus E2-NS2 region: identification of p7 and two distinct E2-specific products with different C termini. J. Virol. 68, 5063–5073.

Lindenbach, B.D., Evans, M.J., Syder, A.J., Wolk, B., Tellinghuisen, T.L., Liu, C.C., Maruyama, T., Hynes, R.O., Burton, D.R., McKeating, J.A., Rice, C.M., 2005. Complete replication of hepatitis C virus in cell culture. Science 309, 623–626.

Lohmann, V., Koch, J.O., Bartenschlager, R., 1996. Processing pathways of the hepatitis C virus proteins. J. Hepatol. 24, 11–19.

Mangia, A., Leandro, G., Helbling, B., Renner, E.L., Tabone, M., Sidoli, L., Caronia, S., Foster, G.R., Zeuzem, S., Berg, T., Di Marco, V., Cino, N., Andriulli, A., 2004. Combination therapy with amantadine and interferon in naive patients with chronic hepatitis C: meta-analysis of individual patient data from six clinical trials. J. Hepatol. 40, 478–483.

Maynard, M., Pradat, P., Bailly, F., Rozier, F., Nemoz, C., Si Ahmed, S.N., Adeleine, P., Trépo, C., 2006. Amantadine triple therapy for non-responder hepatitis C patients. Clues for controversies (ANRS HC 03 BITRI). J. Hepatol. 44, 484–490.

Mihm, U., Grigorian, N., Welsch, C., Herrmann, E., Kronenberger, B., Teuber, G., von Wagner, M., Hofmann, W.P., Albrecht, M., Lengauer, T., Zeuzem, S., Sarrazin, C., 2006. Amino acid variations in hepatitis C virus p7 and sensitivity to antiviral combination therapy with amantadine in chronic hepatitis C. Antivir. Ther. 11, 507–519.

Mizushima, H., Hijikata, M., Asabe, S., Hirota, M., Kimura, K., Shimotohno, K., 1994. Two hepatitis C virus glycoprotein E2 products with different C termini. J. Virol. 68, 6215–6222.

Moradpour, D., Gosert, R., Egger, D., Penin, F., Blum, H.E., Bienz, K., 2003. Membrane association of hepatitis C virus nonstructural proteins and identification of the membrane alteration that harbors the viral replication complex. Antiviral Res. 60, 103–109.

Muzi, F., Orlando, G., Ielpo, B., Anselmo, A., Sabato Ceraldi, S., de'Liguori Carino, N., Manzia, T., D'Andria, D., Tariciotti, L., Angelico, M., Tisone, G., 2005. Amantadine monotherapy is ineffective in the treatment of hepatitis C virus recurrence in the post-liver transplantation setting. Transplant. Proc. 37, 1705–1707.

Okada, A., Miura, T., Takeuchi, H., 2001. Protonation of histidine and histidine–tryptophan interaction in the activation of the M2 ion channel from influenza A virus. Biochemistry 40, 6053–6060.

Park, S.C., Kim, J.Y., Shin, S.O., Jeong, C.Y., Kim, M.H., Shin, S.Y., Cheong, G.W., Park, Y., Hahm, K.S., 2006. Investigation of toroidal pore and oligomerization by melittin using transmission electron microscopy. Biochem. Biophys. Res. Commun. 343, 222–228.

Patargias, G., Zitzmann, N., Dwek, R., Fischer, W.B., 2006. Protein–protein interactions: modeling the hepatitis C virus ion channel p7. J. Med. Chem. 49, 648–655.

Pavlovic, D., Neville, D.C., Argaud, O., Blumberg, B., Dwek, R.A., Fischer, W.B., Zitzmann, N., 2003. The hepatitis C virus p7 protein forms an ion channel that is inhibited by long-alkyl-chain iminosugar derivatives. Proc. Natl. Acad. Sci. U. S. A. 100, 6104–6108.

Pawlotsky, J.M., 2000. Hepatitis C virus resistance to antiviral therapy. Hepatology 32, 889–896.

Pinto, L.H., Dieckmann, G.R., Gandhi, C.S., Papworth, C.G., Braman, J., Shaughnessy, M.A., Lear, J.D., Lamb, R.A., DeGrado, W.F., 1997. A functionally defined model for the M2 proton channel of influenza A virus suggests a mechanism for its ion selectivity. Proc. Natl. Acad. Sci. U. S. A. 94, 11301–11306.

Premkumar, A., Wilson, L., Ewart, G.D., Gage, P.W., 2004. Cation-selective ion channels formed by p7 of hepatitis C virus are blocked by hexamethylene amiloride. FEBS Lett. 557, 99–103.

Premkumar, A., Dong, X., Haqshenas, G., Gage, P.W., Gowans, E.J., 2006. Amantadine inhibits the function of an ion channel encoded by GB virus B, but fails to inhibit virus replication. Antivir. Ther. 11, 289–295.

Sakaguchi, T., Leser, G.P., Lamb, R.A., 1996. The ion channel activity of the influenza virus M2 protein affects transport through the Golgi apparatus. J. Cell. Biol. 133, 733–747.

Sakai, A., Claire, M.S., Faulk, K., Govindarajan, S., Emerson, S.U., Purcell, R.H., Bukh, J., 2003. The p7 polypeptide of hepatitis C virus is critical for infectivity and contains functionally important genotype-specific sequences. Proc. Natl. Acad. Sci. U. S. A. 100, 11646–11651.

Simmonds, P., 2004. Genetic diversity and evolution of hepatitis C virus—15 years on. J. Gen. Virol. 85, 3173–3188.

Simmonds, P., Bukh, J., Combet, C., Deleage, G., Enomoto, N., Feinstone, S., Halfon, P., Inchauspe, G., Kuiken, C., Maertens, G., Mizokami, M., Murphy, D.G., Okamoto, H., Pawlotsky, J.M., Penin, F., Sablon, E., Shin, I.T., Stuyver, L.J., Thiel, H.J., Viazov, S., Weiner, A.J., Widell, A., 2005. Consensus proposals for a unified system of nomenclature of hepatitis C virus genotypes. Hepatology 42, 962–973.

Takikawa, S., Engle, R.E., Emerson, S.U., Purcell, R.H., St Claire, M., Bukh, J., 2006. Functional analyses of GB virus B p13 protein: development of a recombinant GB virus B hepatitis virus with a p7 protein. Proc. Natl. Acad. Sci. U. S. A. 103, 3345–3350.

Tscherne, D.M., Jones, C.T., Evans, M.J., Lindenbach, B.D., McKeating, J.A., Rice, C.M., 2006. Time- and temperature-dependent activation of hepatitis C virus for low-pH-triggered entry. J. Virol. 80, 1734–1741.

Wakita, T., Pietschmann, T., Kato, T., Date, T., Miyamoto, M., Zhao, Z., Murthy, K., Habermann, A., Krausslich, H.G., Mizokami, M., Bartenschlager, R., Liang, T.J., 2005. Production of infectious hepatitis C virus in tissue culture from a cloned viral genome. Nat. Med. 11, 791–796.

Wang, C., Takeuchi, K., Pinto, L.H., Lamb, R.A., 1993. Ion channel activity of influenza A virus M2 protein: characterization of the amantadine block. J. Virol. 67, 5585–5594.

Wang, C., Lamb, R.A., Pinto, L.H., 1995. Activation of the M2 ion channel of influenza virus: a role for the transmembrane domain histidine residue. Biophys. J. 69, 1363–1371.

Zhong, J., Gastaminza, P., Cheng, G., Kapadia, S., Kato, T., Burton, D.R., Wieland, S.F., Uprichard, S.L., Wakita, T., Chisari, F.V., 2005. Robust hepatitis C virus infection in vitro. Proc. Natl. Acad. Sci. U. S. A. 102, 9294–9299.